80. Structural Study of Pinacidil, a Potassium-Channel Opener Belonging to the Chemical Class of *N*-Alkyl-*N''*-cyano-*N'*-pyridylguanidines

by **Bernard Pirotte**[a]*, **Léon Dupont**[b]), **Pascal de Tullio**[a]), **Bernard Masereel**[a]), **Marc Schynts**[a]), and **Jacques Delarge**[a])

[a]) Chimie Pharmaceutique, Institut de Pharmacie, F1, Université de Liège, rue Fusch, 3, B-4000 Liège
[b]) Cristallographie, Institut de Physique, B5, Université de Liège, Sart-Tilman, B-4000 Liège

(22.XII.92)

The crystal structure of the potassium-channel opener (*R,S*)-pinacidil (**2**) was determined by X-ray crystallography. Its *N',N''*-disubstituted *N*-cyanoguanidine fragment was found to exhibit an unusual (*Z,Z*)-conformation. X-Ray and NMR data obtained with **2** are consistent with the predominance of the 4-aminopyridine species over an iminopyridine tautomer in the solid state and in solution. These new structural informations may help further comparative studies of **2** and other potassium-channel openers in elucidating structure-activity relationships.

Introduction. – Potassium channels comprise the most diverse groups of ion channels so far investigated. Among those, the so-called ATP-sensitive K^+ channels (K_{ATP} channels) found considerable interest, since recent studies demonstrated their particular role in physiological processes such as regulation of insulin secretion from pancreatic β-cells [1] and cell-protective response to anoxic conditions [2–4]. K_{ATP} channels were identified in various tissues such as the cardiac muscle [5], pancreatic β-cells [6], skeletal muscle [7], smooth muscle [8], and central neurons [9].

Over the past few years, the number of chemical agents with K^+ channel opening properties has greatly expanded [10] [11]. They can be used as powerful therapeutic agents for multiple indications [11] [12]. They are separated into distinct chemical classes, typically exemplified by cromakalim (**1**; benzopyran), pinacidil (**2**; alkyl-cyano-pyridylguanidine), diazoxide (**3**; benzothiadiazine), nicorandil (**4**; pyridyl-substituted nitro compound), minoxidil sulfate (**5**; pyrimidine derivative), and RP 49356 (**6**; pyridyl-substituted thioformamide) [10].

All these compounds act as hypotensors as a result of their K^+ channel opening properties on vascular smooth muscles [10] [12]. Although the K_{ATP} channel has generally been suggested to be the target of these different compounds, the unique implication of this particular K^+ channel type in their vasorelaxant activity still remains controversial in some instances [12–14]. Moreover, since the potency of the different compounds may vary considerably with tissue localization of the K_{ATP} channels, a heterogeneous population of channels was suggested [12] [15]. For the three best studied K^+-channel openers, the rank order of potency for vascular smooth muscle relaxation was found to be cromakalim (**1**) > pinacidil (**2**) > diazoxide (**3**) [16] [17], whereas for their activity on insulin-secreting cells, the order was **3** > **2** > **1** [18–20]. Since **3** acts as the more efficient activator of the pancreatic K_{ATP} channel [18], this channel appears to be distinct from the other putative K_{ATP} channels so far investigated. (*R,S*)-Pinacidil (**2**) was recently reported

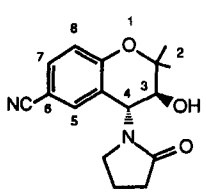

1 cromakalim

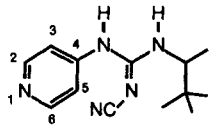

2 pinacidil

3 diazoxide

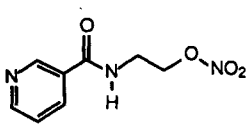

4 nicorandil

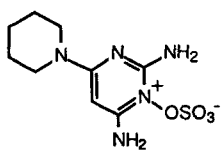

5 minoxidil sulfate

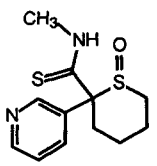

6 RP 49356

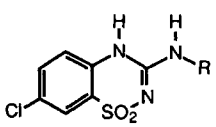

7

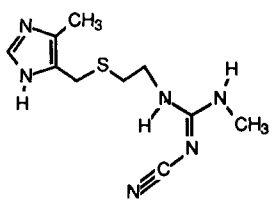

8 cimetidine

to exert a similar pharmacological profile on insulin-secreting cells, but at higher doses than those required for vasorelaxant effect [19]. Recent studies also suggested that **3** and **2** could exert their activity on the K_{ATP} channel after interaction with a common binding site on the pancreatic β-cells [21] [22].

Structure-activity relationships of K^+-channel openers showed that, in the benzopyran series (see **1**), the benzo moiety bearing an electron-withdrawing group (typically CN) at C(6) can be replaced with a pyrido moiety (N in the 6-position, see **1**) without loss of biological activity [10] [23]. Moreover, cromakalim analogs bearing an electron-withdrawing substituent at C(7) in place of C(6) retain hypotensive activity [23]. Substitution in the 8- and 5-positions is less favourable [23]. In the alkyl-cyano-pyridylguanidine series (see **2**), the pyrid-4-yl substituent can be replaced with a pyrid-3-yl or with a 4-cyanophenyl moiety with retention of biological activity [10]. For benzothiadiazine derivatives (see **3**), an electron-withdrawing group (typically Cl, Br, CF_3) at C(6) and/or C(7) enhance hypotensive activity [10] [24]. The 5- and 8-positions are less favourable [24].

In summary, these three classes of compounds, which seem to be structurally different, have an aromatic ring in common on which the critical positions for an electron-withdrawing substituent (or N-atom of the pyridine isostere) are topologically superimposable. Assuming that the pyridine ring might be nearly coplanar with the guanidine

moiety, **2** could be regarded as a fairly good structural analog of **3**. A better comparison could be made with 3-alkylamino derivatives **7** of diazoxide which are known to be potent antihypertensive agents themselves [25].

The actual informations in the literature related to the geometry of pinacidil (**2**) are clearly insufficient. Therefore, the aim of the present work is to reveal unknown aspects in this field. Such information may help further investigations on structural comparisons between different potassium-channel openers and highlight some common pharmacological properties.

Results and Discussion. – *Crystallographic Results Obtained with (*R,S*)-Pinacidil* (**2**). *Fig. 1* shows a thermal-ellipsoid stereoscopic ORTEP plot of (*RS*)-pinacidil (**2**) and the atomic numbering [26]. A stereoscopic PLUTO [27] view of the unit cell is represented in *Fig. 2*.

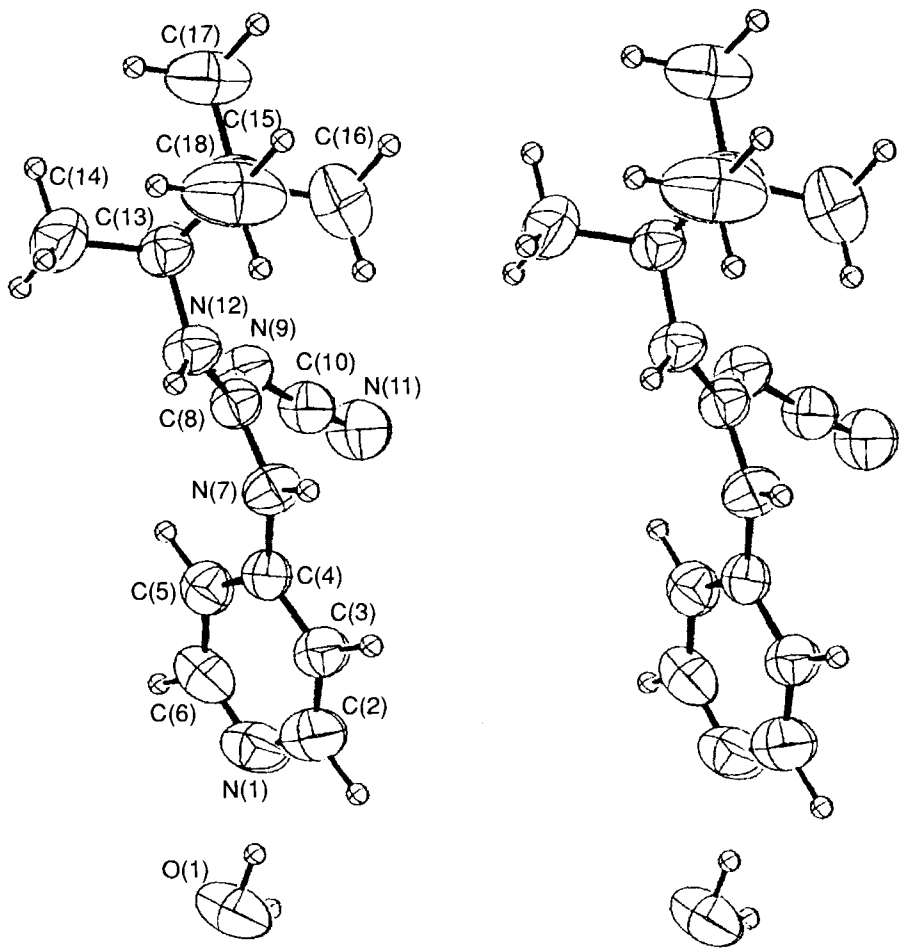

Fig. 1. *ORTEP stereoscopic view of pinacidil* (**2**) *in the crystal.* Arbitrary numbering.

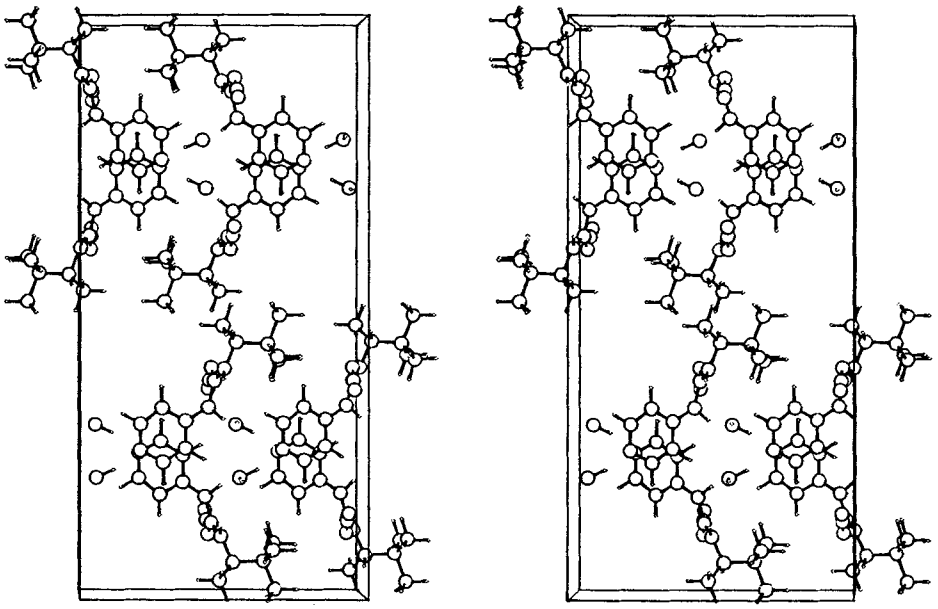

Fig. 2. *PLUTO stereoscopic view of pinacidil* (**2**) *along the* a *axis*

The individual bond lengths and angles (*Table 1*) do not differ significantly from the expected values. The pyridine ring is planar within experimental error. Some characteristic dihedral angles are given in *Table 2*. There are several intermolecular H-bonds involving O(1) (H_2O) and N-atoms of pinacidil (*Table 1*). The A–H···B associated angles are: O(1)–H(102)···N(1), 160(3)°; N(7^{ii})–H(7^{ii})···O(1), 170(3)°; N(12^{iii})–H(12^{iii})···N(11), 166(3)°. The geometry of O(1)–H(101)···N(11^{i}) is far from linear (114(3)°), and the distance N(11^{i})–H(101) (2.51(2) Å) is only slightly below the sum of their *van-der-Waals* radii (> 2.6 Å [28] [29]). Thus, the existence of a H-bond between O(1) and N(11) is questionable.

Chemical-Structure Considerations of N-*Cyano*-N′-*pyridylguanidines. N′,N″*-Disubstituted *N*-cyanoguanidines may exhibit different tautomeric forms (see **A**–**C**, *Scheme 1*). The predominance of the cyanoimino tautomer **B** was established by many physicochemical studies on cyanoguanidines [30] [31]. This predominance was also found in the crystal structure of pinacidil (**2**): The shortest C–N bond in the guanidine group carries the C≡N group (C(8)–N(7), 1.373 Å; C(8)–N(9), 1.316 Å; C(8)–N(12), 1.329 Å). In most of the 25 guanidines retrieved from the *Cambridge Crystallographic Data File*, there are no significant differences between the three C–N distances; in crystals, the C–N bonds are widely delocalized. *E.g.*, in (D_4)dicyanodiamide (= (D_4)cyanoguanidine) [32], the values of the three C–N distances are 1.328, 1.329, and 1.330(2) Å. The guanidine moiety has a planar geometry in most of these examples.

Due to restricted rotation about their C–N bonds, eight different conformations may theoretically be adopted by *N′,N″*-disubstituted *N*-cyanoguanidines (see **D**–**K**, $R^1 \neq R^2$, *Scheme 2*). Among them, **D** and **I** should be energetically the most favourable, from the point of view of the steric interactions between the substituents and the C≡N group.

Table 1. *Distances* [Å] *and Bond Angles* [°] *of Pinacidil* (**2**) *with e.s.d.'s*

C(2)–N(1)	1.335 (4)	N(11)–C(10)	1.151 (3)
C(6)–N(1)	1.333 (4)	C(13)–N(12)	1.456 (3)
C(3)–C(2)	1.358 (4)	C(14)–C(13)	1.517 (5)
C(4)–C(3)	1.388 (4)	C(15)–C(13)	1.545 (4)
C(5)–C(4)	1.391 (4)	C(16)–C(15)	1.534 (5)
N(7)–C(4)	1.395 (3)	C(17)–C(15)	1.537 (5)
C(6)–C(5)	1.387 (4)	C(18)–C(15)	1.526 (5)
C(8)–N(7)	1.373 (3)	O(1)–N(1)	2.697 (4)[a]
N(9)–C(8)	1.316 (3)	O(1)···N(11^{i})[b]	3.044 (4)[a]
N(12)–C(8)	1.329 (3)	O(1)···N(7^{ii})[b]	2.737 (4)[a]
C(10)–N(9)	1.316 (3)	N(11)···N(12^{iii})[b]	3.107 (4)[a]
C(6)–N(1)–C(2)	116.6 (3)	C(13)–N(12)–C(8)	125.3 (2)
C(3)–C(2)–N(1)	124.0 (3)	C(14)–C(13)–N(12)	108.2 (2)
C(4)–C(3)–C(2)	119.3 (3)	C(15)–C(13)–N(12)	111.6 (2)
C(5)–C(4)–C(3)	118.3 (2)	C(15)–C(13)–C(14)	115.2 (2)
N(7)–C(4)–C(3)	118.4 (2)	C(16)–C(15)–C(13)	108.5 (3)
N(7)–C(4)–C(5)	123.2 (2)	C(17)–C(15)–C(13)	108.4 (3)
C(6)–C(5)–C(4)	117.6 (3)	C(17)–C(15)–C(16)	108.8 (3)
C(5)–C(6)–N(1)	124.3 (3)	C(18)–C(15)–C(13)	111.5 (3)
C(8)–N(7)–C(4)	126.9 (2)	C(18)–C(15)–C(16)	110.5 (3)
N(9)–C(8)–N(7)	125.0 (2)	C(18)–C(15)–C(17)	109.2 (3)
N(12)–C(8)–N(7)	115.2 (2)	N(1)–O(1)···N(7^{ii})[b]	119.9 (2)[a]
N(12)–C(8)–N(9)	119.8 (2)	N(7^{ii})–O(1)···N(11^{i})[b]	83.9 (2)[a]
C(10)–N(9)–C(8)	120.0 (2)	N(1)–O(1)···N(11^{i})[b]	152.1 (2)[a]
N(11)–C(10)–N(9)	172.5 (3)	C(10)–N(11)···C(12^{iii})[b]	135.3 (2)[a]

[a]) These values correspond to H-bonds.

[b]) Symmetry code: *i*: $(1-x, -0.5+y, 0.5-z)$; *ii*: $(-x, -0.5+y, 0.5-z)$; *iii*: $(1+x, y, z)$.

Table 2. *Some Dihedral Angles* [°] *for Pinacidil* (**2**) *with e.s.d.'s*

C(5)–C(4)–N(7)–C(8)	–14.4 (3)	H(N7)–N(7)–C(8)–N(12)	–25.2 (7)
C(5)–C(4)–N(7)–H(N7)	149.6 (7)	N(7)–C(8)–N(12)–H(N12)	–12.9 (7)
C(4)–N(7)–C(8)–N(9)	–42.8 (3)	N(9)–C(8)–N(12)–C(13)	–10.2 (3)
N(7)–C(8)–N(9)–C(10)	–18.2 (3)	C(8)–N(12)–C(13)–C(15)	–103.9 (3)
N(7)–C(8)–N(12)–C(13)	167.8 (3)	N(12)–C(13)–C(15)–C(17)	176.0 (3)

Scheme 1

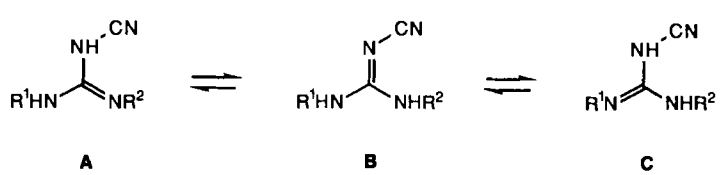

A **B** **C**

Seven crystal structures containing the *N′,N″*-disubstituted *N*-cyanoguanidine cimetidine (**8**), a H_2-receptor antagonist, show that they actually represent the (*E,Z*)-forms **D** [33] or **I** [34]. Of particular interest is the surprising (*Z,Z*)-conformation **J** adopted by (*R,S*)-pinacidil (**2**) in the crystal (R^1 = pyrid-4-yl). It is known that 4-aminopyridines

Scheme 2

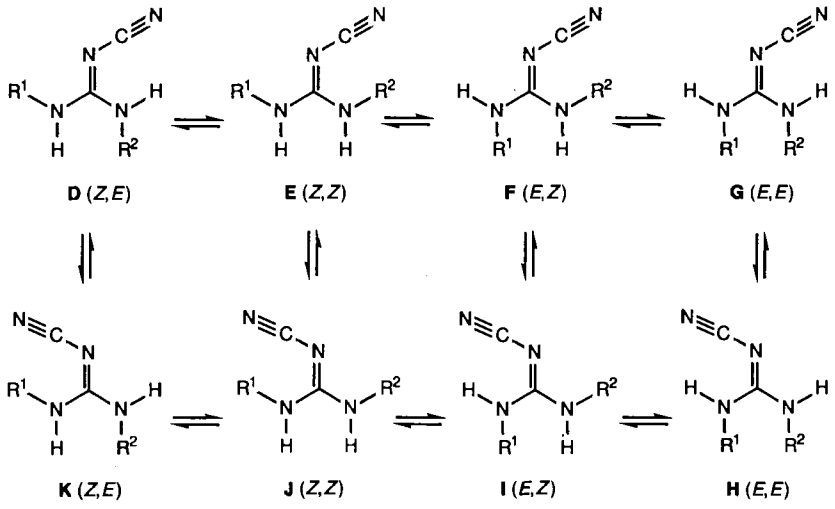

Scheme 3

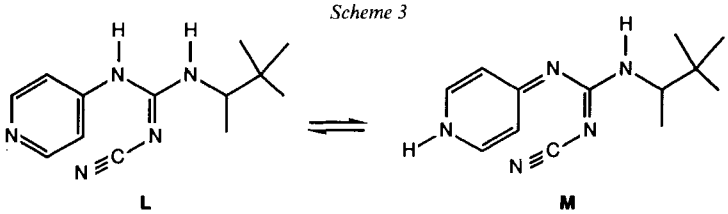

co-exist with an iminopyridine species (see, *e.g.*, **M** in *Scheme 3*), and such an equilibrium was recently reported for cyano-(pyrid-4-yl)guanidine compounds related to **2** [35]. However, crystallographic and NMR data obtained with **2** are consistent with a predominance of the 4-aminopyridine species **L** (*Scheme 3*).

In fact, ^{1}H-NMR signals for the aromatic protons of **2** recorded in different solvents ($CDCl_3$, (D_6)DMSO, (D_6)DMSO/D_2O 2:1 (*v/v*)) at room temperature were found to be sharp absorptions with well-resolved couplings[1]). The (D_6)DMSO/D_2O solvent was chosen for the examination of **2** in a partially hydrated medium, since the low solubility of **2** in H_2O in its non-ionized form (that expected at physiological pH) does not permit the NMR recording in pure D_2O. Interesting low-temperature NMR studies (223 K; $CDCl_3$,

[1]) The ^{1}H-NMR chemical shifts (δ) of **2** (for numbering, see *Fig. 1*) were determined on a *Bruker-AW80* spectrometer at room temperature. ^{1}H-NMR ($CDCl_3$, TMS): 0.90 (*s*, Me_3C); 1.10 (*d*, Me); 3.87 (*dq*, H–C(13)); 5.40 (*d*, NH(12)); 7.13 (*d*, H–C(3), H–C(5)); 8.45 (*d*, H–C(2), H–C(6)). ^{1}H-NMR ((D_6)DMSO, HMDS): 0.82 (*s*, Me_3C); 1.00 (*d*, Me); 3.82 (*dq*, H–C(13)); 7.05 (*d*, H–C(3), H–C(5)); 7.30 (*d*, NH(12)); 8.25 (*d*, H–C(2), H–C(6)); 9.20 (br. *s*, NH(7)); these data are closely related to those reported for **2** in (D_6)DMSO (TMS) [36]. ^{1}H-NMR ((D_6)DMSO/D_2O, sodium (trimethylsilyl)propanoate): 0.90 (*s*, Me_3C); 1.15 (*d*, Me); 3.90 (*q*, H–C(13)); 7.20 (*d*, H–C(3), H–C(5)); 8.35 (*d*, H–C(2), H–C(6)).

(D_6)DMSO) conducted with *N*-cyano-*N'*-(pyrid-4-yl)guanidine analogs of **2** revealed new peaks located close to the initial aromatic-proton absorptions and arising from the co-existence in solution of two molecular species in slow exchange [35]. For **2**, the aminopyridine species was found to be clearly predominant [35].

The bond length C(4)–N(7) obtained for **2** from X-ray data does not exhibit a clear double-bond character. The angle C(6)–N(1)–C(2) (116.6(3)°) and the distances C(2)–N(1) and C(6)–N(1) are those found in pyridine [37] [38]. Moreover, the difference map clearly shows H-atom peaks near N(7) and N(12). All these data exclude predominance of the iminopyridine species in the solid state of **2**.

The atomic distances in the guanidine moiety of **2** show stronger electron delocalization between N(12)–C(8)–N(9) than between C(4)–N(7)–C(8). Moreover, the atomic distances C(8)–N(12) (1.329 Å) and N(12)–C(13) (1.456 Å) corroborate the sp^2 character of the atom N(12) [38]; the situation is less clear for N(7). However, the sum of the three bond angles around N(7) (358.3(7)°) and N(12) (360.0(7)°) confirms the sp^2 geometry of these two guanidine N-atoms, with a slight distortion for N(7). Bond length and geometry distortion for N(7) could result from the strong steric crowding between the C≡N and the pyridyl groups and is probably associated with a partial delocalization of the lone-pair electrons of N(7) into the pyridine ring. In fact, a better coplanarity of N(7) with the pyridine ring rather than with the guanidine moiety is observed (compare C(5)–C(4)–N(7)–C(8) (−14.4°) and C(4)–N(7)–C(8)–N(9) (−42.8°) in *Table 2*) and could result from the preferential delocalization of the lone-pair electrons of N(7) into the pyridine ring.

Experimental Part

X-Ray Crystal Structure of N-*Cyano*-N'-*(pyridin-4-yl)*-N''-*(1,2,2-trimethylpropyl)guanidine* (= *Pinacidil*; **2**). Colorless crystals were obtained by slow evaporation of a H_2O/MeOH soln. at 290 K. Crystallographic data: $C_{13}H_{19}N_5 \cdot H_2O$, $Mr = 263.34$, orthorhombic, space group *Pbca*, $a = 7.2736(6)$, $b = 14.1967(18)$, $c = 29.2046(66)$ Å, $V = 3015.7(1)$ Å^3, $Z = 8$, $D_x = 1.160$ g·cm^{-3}, $F(000) = 1136$, Cu$K\alpha$, $\lambda = 1.5418$ A, $\mu = 5.50$ cm^{-1}. The crystal studied was prismatic with dimensions 0.27 × 0.53 × 0.30 mm. The intensities were collected at 290 K on a *Siemens* automatic diffractometer, with CuK_α radiation and a graphite monochromator. $\theta_{max} = 58°$ (ω scan). The cell parameters were refined by least squares from 44 reflections in the θ range 36–40°. The variations of the two standard reflections are $8247 \leqslant F_o(080) \leqslant 8768$ and $8209 \leqslant F_o(0.80) \leqslant 8853$. The intensities were corrected for *Lorentz* and polarization factors. Decay and absorption corrections (by semiempirical method) were also applied. The minimum and maximum transmission factors are 0.95 and 0.99, resp. The structure was determined by direct methods with SHELXS 86 [39]. All positional parameters and anisotropic thermal parameters for non H-atoms were refined with SHELX 76 [40] by the full-matrix least-squares method. The H-atom positions were calculated except for H(N7), H(N12), and H(H_2O), whose positions were obtained from the difference map. A global isotropic thermal parameter B was refined for the H (CH; 6.4(3) Å^2) and for the H (CH_3; 11.1(3) Å^2). The B of H (H_2O) was fixed at 6.3 Å^2. Scattering factors were taken from SHELX 76 data. Final discrepancy indices $R = 0.050$ for 1572 observed reflections ($I > \sigma(I)$). $wR = 0.056$ where $w = 1/[\sigma^2(F) + 0.023\ F^2]$. Maximum $\Delta/\sigma = 0.02$ in final least-squares cycle. Final difference *Fourier* map showed no residual greater than 0.14 eÅ^{-3}. The lists of fractional atomic coordinates of cell atoms, equivalent temperature factors, structure amplitudes, and anisotropic thermal parameters were deposited with the *Cambridge Crystallographic Data Center*.

REFERENCES

[1] F.M. Ashcroft, *Annu. Rev. Neurosci.* **1988,** *11,* 97.
[2] G.J. Grover, J.R. McCullouch, D.E. Henry, M.L. Conder, P.G. Sleph, *J. Pharmacol. Exp. Ther.* **1989,** *251,* 98.
[3] K.P.S.J. Murphy, S.A. Greenfield, *Exp. Brain Res.* **1991,** *84,* 355.
[4] D. Escande, I. Cavero, *Trends Pharmacol. Sci.* **1992,** *13,* 269.
[5] A. Noma, *Nature (London)* **1983,** *305,* 147.
[6] D.L. Cook, C.N. Hales, *Nature (London)* **1984,** *311,* 271.
[7] A.E. Spruce, N.B. Standen, P.R. Stanfield, *Nature (London)* **1985,** *316,* 736.
[8] N.B. Standen, J.M. Quayle, N.W. Davies, J.E. Brayden, Y. Huang, M.T. Nelson, *Science* **1989,** *245,* 177.
[9] H. Bernardi, M. Fosset, M. Lazdunski, *Proc. Natl. Acad. Sci. U.S.A.* **1988,** *85,* 9816.
[10] G. Edwards, A.H. Weston, *Trends Pharmacol. Sci.* **1990,** *11,* 417.
[11] D.W. Robertson, M.I. Steinberg, *J. Med. Chem.* **1990,** *33,* 1529.
[12] S.D. Longman, T.C. Hamilton, *Med. Res. Rev.* **1992,** *12,* 73.
[13] T.L. Grant, J.S. Zuzack, *J. Pharmacol. Exp. Ther.* **1991,** *259,* 1158.
[14] A.H. Weston, G. Edwards, *Biochem. Pharmacol.* **1992,** *43,* 47.
[15] M. Gopalakrishnan, D.E. Johnson, R.A. Janis, D.J. Triggle, *J. Pharmacol. Exp. Ther.* **1991,** *257,* 1162.
[16] T.C. Hamilton, A.H. Weston, *Gen. Pharmacol.* **1989,** *20,* 1.
[17] D.T. Newgreen, K.M. Bray, A.D. McHarg, A.H. Weston, S. Duty, B.S. Brown, P.B. Kay, G. Edwards, J. Longmore, J.S. Southerton, *Br. J. Pharmacol.* **1990,** *100,* 605.
[18] M.G. Garrino, T.D. Plant, J.C. Henquin, *Br. J. Pharmacol.* **1989,** *98,* 957.
[19] P. Lebrun, V. Devreux, M. Hermann, A. Herchuelz, *J. Pharmacol. Exp. Ther.* **1989,** *250,* 1011.
[20] P. Lebrun, M.-H. Antoine, V. Devreux, M. Hermann, A. Herchuelz, *J. Pharmacol. Exp. Ther.* **1990,** *255,* 948.
[21] M. Schwanstecher, C. Brandt, S. Behrends, U. Schaupp, U. Panten, *Br. J. Pharmacol.* **1992,** *106,* 295.
[22] M. Schwanstecher, 'Ion Channel Structure and Modulation. New Possibilities for Drug Development', IBC Technical Services Ltd., London, 1992.
[23] J.M. Evans, G. Stemp, 'Potassium Channels '90. Structure, Modulation, and Clinical Exploitation', IBC Technical Services Ltd., London, 1990.
[24] J.G. Topliss, M.D. Yudis, *J. Med. Chem.* **1972,** *15,* 394.
[25] H. Wollweber, H. Horstmann, K. Stoepel, B. Garthoff, W. Puls, H.P. Krause, G. Thomas, *Arzneim.-Forsch./Drug Res.* **1981,** *31,* 279.
[26] C.K. Johnson, 'ORTEP II', 'A Fortran Thermal-Ellipsoïd Plot Program for Crystal Structure Illustrations', ORNL-3794, revised, Oak Ridge, Tennessee, USA, 1972.
[27] 'PLUTO, Cambridge Structural Database System', University of Cambridge, U.K., 1978.
[28] Z. Rahim, B.N. Barman, *Acta Crystallogr., Sect. A* **1978,** *34,* 761.
[29] S.C. Nyburg, C.H. Faerman, *Acta Crystallogr., Sect. B* **1985,** *41,* 274.
[30] G.T. Durant, J.C. Emmett, R.C. Ganellin, P.D. Miles, M.E. Parsons, H.D. Prain, G.R. White, *J. Med. Chem.* **1977,** *20,* 901.
[31] R.D. Bach, J.J.W. McDouall, A.L. Owensby, H.B. Schlegel, J.W. Holubka, J.C. Ball, *J. Phys. Org. Chem.* **1991,** *4,* 125.
[32] N.V. Rannev, R.P. Ozerov, I.D. Datt, A.N. Kshnyakina, *Kristallografya* **1966,** *11,* 175.
[33] M. Shibata, M. Kagawa, K. Morisaka, T. Ishida, M. Inohue, *Acta Crystallogr., Sect. C* **1983,** *39,* 1855.
[34] B. Kojic-Prodic, Z. Ruzic-Toros, N. Bresciani-Pahor, L. Randaccio, *Acta Crystallogr., Sect. B* **1980,** *36,* 1223.
[35] P.W. Manley, U. Quast, *J. Med. Chem.* **1992,** *35,* 2327.
[36] H.J. Petersen, C.K. Nielsen, E. Arrigoni-Martelli, *J. Med. Chem.* **1978,** *21,* 773.
[37] L. Dupont, O. Dideberg, M. Vermeire, *Acta Crystallogr., Sect. B* **1979,** *35,* 150.
[38] F.H. Allen, O. Kennard, D.G. Watson, L. Brammer, A.G. Orpen, *J. Chem. Soc., Perkin Trans. 2* **1987,** S1.
[39] G.M. Sheldrick, 'SHELXS 86, Program for the Resolution of Crystal Structures', University of Cambridge, U.K., 1986.
[40] G.M. Sheldrick, 'SHELX 76, Program for the Determination of Crystal Structures', University of Cambridge, U.K., 1976.